THE JOURNAL OF BIOLOGICAL CHEMISTRY Vol. 280, No. 9, Issue of March 4, pp. 8452–8463, 2005

Printed in U.S.A.

Modulation of the Actin Cytoskeleton via Gelsolin Regulates Vacuolar H^+-ATPase Recycling*

Received for publication, November 10, 2004
Published, JBC Papers in Press, December 9, 2004, DOI 10.1074/jbc.M412750200

Valérie Beaulieu‡, Nicolas Da Silva‡, Nuria Pastor-Soler‡, Christopher R. Brown‡, Peter J. S. Smith§, Dennis Brown‡¶, and Sylvie Breton‡¶‖

From the ‡Program in Membrane Biology, Massachusetts General Hospital, Charlestown, Massachusetts 02129, the ¶Department of Medicine, Harvard Medical School, Boston, Massachusetts 02215, and the §BioCurrents Research Center, Marine Biological Laboratory, Woods Hole, Massachusetts 02543

The role of the actin cytoskeleton in regulating membrane protein trafficking is complex and depends on the cell type and protein being examined. Using the epididymis as a model system in which luminal acidification is crucial for sperm maturation and storage, we now report that modulation of the actin cytoskeleton by the calcium-activated actin-capping and -severing protein gelsolin plays a key role in regulating vacuolar H^+-ATPase (V-ATPase) recycling. Epididymal clear cells contain abundant V-ATPase in their apical pole, and an increase in their cell-surface V-ATPase expression correlates with an increase in luminal proton secretion. We have shown that apical membrane accumulation of V-ATPase is triggered by an elevation in cAMP following activation of bicarbonate-regulated soluble adenylyl cyclase in response to alkaline luminal pH (Pastor-Soler, N., Beaulieu, V., Litvin, T. N., Da Silva, N., Chen, Y., Brown, D., Buck, J., Levin, L. R., and Breton, S. (2003) *J. Biol. Chem.* 278, 49523–49529). Here, we show that clear cells express high levels of gelsolin, indicating a potential role in the functional activity of these cells. When jasplakinolide was used to overcome the severing action of gelsolin by polymerizing actin, complete inhibition of the alkaline pH- and cAMP-induced apical membrane accumulation of V-ATPase was observed. Conversely, when gelsolin-mediated actin filament elongation was inhibited using a 10-residue peptide (PBP10) derived from the phosphatidylinositol 4,5-bisphosphate-binding region (phosphoinositide-binding domain 2) of gelsolin, significant V-ATPase apical membrane mobilization was induced, even at acidic luminal pH. In contrast, the calcium chelator 1,2-bis(2-aminophenoxy)ethane-*N*,*N*,*N*′,*N*′-tetraacetic acid tetrakis(acetoxymethyl ester) and the phospholipase C inhibitor U-73122 inhibited the alkaline pH-induced V-ATPase apical accumulation. Thus, maintenance of the actin cytoskeleton in a depolymerized state by gelsolin facilitates calcium-dependent apical accumulation of V-ATPase in response to luminal pH alkalinization. Gelsolin is present in other cell types that express the V-ATPase in their plasma membrane and recycling vesicles, including kidney intercalated cells and osteoclasts. Therefore, modulation of the actin cortex by this severing and capping protein may represent a common mechanism by which these cells regulate their rate of proton secretion.

The actin cytoskeleton is a dynamic structure that is involved in a variety of cellular processes, including cell motility (1–6), division (7), adhesion (8), and vesicle trafficking (9–20). In eukaryotic cells, a dense sheet of polymerized actin adjacent to the plasma membrane forms the actin cortex. The role of the cortical actin in regulating vesicle trafficking is extremely complex, and numerous studies have shown that depolymerization of the actin cytoskeleton can either facilitate or impair vesicle recycling. This topic has been extensively reviewed (20, 21), and the following examples illustrate the variability of results obtained upon actin cytoskeleton modification. Orci *et al.* (13) were among the first to demonstrate that the actin-depolymerizing agent cytochalasin can either stimulate or inhibit exocytosis depending on the experimental conditions used. Actin depolymerization enhances catecholamine secretion in adrenal chromaffin cells (22, 23), suggesting that the actin cortex can form a barrier for exocytic vesicles. Although a similar stimulation of exocytosis was observed upon moderate actin depolymerization in pancreatic acinar cells, severe depletion of F-actin inhibited exocytosis in these cells (18), indicating the need for a minimal amount of polymerized actin. In intact muscle, the insulin-stimulated cell-surface mobilization of GLUT4 is inhibited after disruption of cortical F-actin (24). In contrast, accumulation of the water channel AQP2 in the plasma membrane of primary cultured kidney collecting duct principal cells occurs after disruption of the actin cytoskeleton (25). Increase in surface expression of AQP2 is promoted by vasopressin in the mammalian kidney and toad bladder (26), and in the latter, this process was shown to be accompanied by depolymerization of the actin cytoskeleton (27). More recently, actin filaments were proposed to facilitate endocytosis of water channels but not to be required for exocytosis in the toad bladder (28). In some cells, disruption of the actin cytoskeleton inhibits apical endocytosis without affecting basolateral endocytosis (29, 30). Another study showed variable effects on receptor-mediated endocytosis after either depolymerization or polymerization of actin filaments in different cell types (31). It therefore appears that opposite effects can be obtained following disruption of the actin cytoskeleton depending on the cell type or the nature of the recycling process examined.

* This work was supported by National Institutes of Health Grants HD40793 (to S. B.), DK38452 (to D. B. and S. B.), DK42956 (to D. B.), P41-RR001395 (to P. J. S. S.), and KO8-HD45524 (to N.P.-S.) and National Research Service Award HD08684 (to N. P.-S.). The work performed in the Microscopy Core Facility of the Massachusetts General Hospital Program in Membrane Biology was supported by Center for the Study of Inflammatory Bowel Disease Grant DK43351 and Boston Area Diabetes and Endocrinology Research Center Award DK57521. The costs of publication of this article were defrayed in part by the payment of page charges. This article must therefore be hereby marked "*advertisement*" in accordance with 18 U.S.C. Section 1734 solely to indicate this fact.

‖ To whom correspondence and reprint requests should be addressed: Program in Membrane Biology, Massachusetts General Hospital East, 149 13th St., Charlestown, MA 02129. Tel.: 617-726-5785; Fax: 617-726-5669; E-mail: sbreton@partners.org.

Remodeling of the actin cytoskeleton is controlled by several intracellular proteins, including the calcium-activated actin-severing proteins villin, gelsolin, fragmin, severin, and adseverin (scinderin) (32, 33). Gelsolin severs actin filaments and caps their fast-growing barbed ends, thereby promoting rapid actin filament fragmentation and blocking their elongation (34, 35). The binding of gelsolin to actin is activated by calcium and by low pH, whereas phosphatidylinositol 4,5-bisphosphate (PIP_2)[1] and some other phosphoinositides remove gelsolin from the barbed ends of actin filaments (36, 37). Two phosphoinositide-binding domains (PBDs) of gelsolin (PBD1 and PBD2; 10–20 amino acids each) have been identified (38). The actin-severing activity of gelsolin is located in the N-terminal half of gelsolin (38). Thus, modulation of the actin cytoskeleton by gelsolin is a regulated and complex process that involves both the severing and capping properties of gelsolin.

Gelsolin was shown to be highly expressed in a variety of cell types involved in active plasma membrane recycling, including osteoclasts, kidney intercalated cells, and spermatozoa (39–41). It was proposed that active remodeling of the actin cytoskeleton by gelsolin might regulate the endo/exocytic activity in these cells. In this study, we show that gelsolin is highly expressed in another cell type involved in active recycling, the clear cells of the epididymis. Furthermore, osteoclasts, kidney intercalated cells, and epididymal clear cells all express high levels of the vacuolar H^+-ATPase (V-ATPase) on intracellular vesicles and the plasma membrane (42–46). Active proton secretion by these cells via the V-ATPase is responsible for bone resorption (osteoclasts) (46, 47), systemic acid/base homeostasis (intercalated cells) (48), and maintenance of sperm in a dormant state during maturation and storage in the epididymis (clear cells) (43).

The V-ATPase is a complex enzyme composed of numerous subunits, some of which are present in multiple copies in each holoenzyme (49, 50). It is ubiquitously expressed in eukaryotic cells, where it is located in intracellular acidic organelles, including lysosomes, the Golgi apparatus, secretory vesicles, and endosomes. In some specialized cells such as osteoclasts, kidney intercalated cells, and epididymal clear cells, the V-ATPase is also expressed in the plasma membrane (46, 48, 51, 52). In these cells, the V-ATPase rapidly recycles between intracellular vesicles and the plasma membrane, and an increase in proton secretion correlates with an increase in V-ATPase surface expression (48, 53–55).

We (59) and others (55–58) have shown that the V-ATPase can bind either directly or indirectly to actin via two of its subunits, B and C, located on the cytoplasmic side of the membrane. The B subunit of the V-ATPase exists in two forms known as B1 and B2. The B1 subunit is predominant in kidney intercalated cells and epididymal clear cells (44, 45, 60), whereas osteoclasts express the B2 isoform (47). These isoforms are highly homologous, and they both bind directly to actin via their cytoplasmic N termini (56, 58). In addition, the B1 subunit, but not the B2 subunit, contains a DTAL motif in its C terminus, which allows for binding to the PDZ domain-containing protein NHERF1 (59). NHERF1, which was originally identified as a cofactor for the regulation of the Na^+/H^+ exchanger NHE3 (61), binds to the ezrin/radixin/moesin family of actin-binding proteins and links many membrane proteins to the actin cytoskeleton (62). Thus, NHERF1 may allow for indirect interaction between V-ATPase and actin. It was proposed that interaction between the V-ATPase and F-actin is required for V-ATPase-dependent proton secretion by osteoclasts (55), but whether this is also the case in other cell types remains to be elucidated. In addition, although the role of the actin cytoskeleton in regulating clathrin-mediated endocytosis is clearly emerging (20, 63), its role in the recycling of V-ATPase, which utilizes unique clathrin- and caveolin-independent mechanisms (51, 64), has not been demonstrated yet.

In this study, we used epididymal clear cells as a model system to examine the role of actin cytoskeleton modulation via gelsolin in regulating V-ATPase-dependent proton secretion. This model allows the study of V-ATPase recycling in intact cells while they reside in their native epithelium. The epididymis establishes a low luminal pH of 6.5–6.8 to maintain spermatozoa in a quiescent state during their maturation and storage in this organ. We have shown previously that clear cells are key players in this acidification process (43). In addition, we have shown that V-ATPase recycling in these cells is strongly dependent on luminal pH and that a bicarbonate-regulated soluble adenylyl cyclase-dependent rise in cAMP in response to alkaline luminal pH induces an accumulation of V-ATPase in the apical membrane, leading to significant elongation of V-ATPase-containing microvilli (65). The resulting increase in proton secretion by clear cells would re-establish the pH of the lumen to its resting acidic value. We now show that polymerization of the actin cytoskeleton inhibits the alkaline pH-induced V-ATPase apical cell-surface mobilization in gelsolin-rich clear cells. In addition, a PIP_2-binding peptide that competes for the binding of PIP_2 with gelsolin, thereby preventing uncapping of gelsolin from actin filament barbed ends, favors the apical membrane accumulation of V-ATPase. We also show that the phospholipase C (PLC) calcium signaling pathway is involved in the regulation of V-ATPase trafficking. These data point to a major role for the actin cytoskeleton-remodeling protein gelsolin in regulating V-ATPase endocytosis, a process that is broadly used by specialized acidifying V-ATPase-expressing cells in various tissues and organs.

EXPERIMENTAL PROCEDURES

Tissue Fixation and Immunofluorescence—Adult male Sprague-Dawley rats (Charles River Laboratories, Wilmington, MA) were anesthetized using an intraperitoneal sodium pentobarbital injection of 10 mg/100 g of body weight. They were then perfused through the left ventricle of the heart with phosphate-buffered saline (PBS; 12 mM phosphate buffer containing 137 mM NaCl and 2.7 mM KCl, pH 7.4), followed by PLP fixative containing 10 mM sodium periodate, 75 mM lysine, 4% paraformaldehyde, and 5% sucrose. Epididymides were harvested and further fixed overnight at 4 °C in PLP fixative. Tissues were then washed in PBS and stored in PBS containing 0.02% sodium azide.

PLP-fixed epididymides were cryoprotected in a solution of 30% sucrose in PBS, and 5-μm cryostat sections were cut and picked up onto Fisher Superfrost Plus microscope slides as described previously (42, 65). Sections were hydrated for 15 min in PBS and treated with 1% SDS, an antigen retrieval technique that we have described previously (66). Nonspecific binding of the antibody was blocked by preincubation of sections with 1% bovine serum album in PBS containing 0.02% sodium azide for 15 min. Sections were then incubated with the primary antibody for 90 min at room temperature, followed by two washes of 5 min in high salt PBS (2.7% NaCl) to reduce nonspecific staining and one wash in normal PBS. The secondary antibody was applied for 1 h at room temperature and washed as described above. Double labeling was performed by subsequent incubation of the sections with additional primary and secondary antibodies.

The primary antibodies used were as follows. Affinity-purified chicken or rabbit antibodies raised against the last 10 C-terminal amino acids (C-GANANRKFLD) of the E subunit of the V-ATPase were used at a 1:5 or 1:50 dilution, respectively, and have been characterized previously (59, 65). A rabbit polyclonal antibody against gelsolin, kindly provided and characterized previously by Dr. David J. Kwiatkowski (39), was used at a 1:1200 dilution. A monoclonal antibody raised

[1] The abbreviations used are: PIP_2, phosphatidylinositol 4,5-bisphosphate; PBD, phosphoinositide-binding domain; V-ATPase, vacuolar H^+-ATPase; PLC, phospholipase C; PBS, phosphate-buffered saline; HRP, horseradish peroxidase; BAPTA-AM, 1,2-bis(2-aminophenoxy)ethane-*N*,*N*,*N*′,*N*′-tetraacetic acid tetrakis(acetoxymethyl ester); CPT-cAMP, 8-(4-chlorophenylthio)-cAMP; sAC, soluble adenylyl cyclase.

against chicken gizzard actin (Chemicon International, Inc., Temecula, CA) was used at a 1:100 dilution. The secondary antibodies used were donkey anti-chicken antibody coupled to fluorescein isothiocyanate (7.5 μg/ml), goat anti-rabbit IgG coupled to Cy3 (2 μg/ml) or fluorescein isothiocyanate (7.5 μg/ml), and goat anti-mouse IgG coupled to Cy3 (2 μg/ml) and were purchased from Jackson ImmunoResearch Laboratories, Inc. (West Grove, PA) . All antibodies were diluted in Dako antibody diluent. The slides were mounted in Vectashield (Vector Laboratories, Burlingame, CA) diluted 1:1 with 1.5 M Tris buffer, pH 8.5. Some slides were mounted in Vectashield containing the DNA marker 4′,6-diamidino-2-phenylindole to stain the nucleus. Images were acquired either with a Hamamatsu Orca charge-coupled device camera mounted on a Nikon E800 epifluorescence microscope using IPLab Spectrum software (Scanalytics, Inc., Fairfax, VA) or with a Zeiss Axioplan microscope equipped with a Radiance 2000 confocal laser scanning system (Bio-Rad). Final images were imported into and printed from Adobe Photoshop.

Western Blotting—Homogenate from total epididymis was resuspended in Laemmli sample buffer (Bio-Rad) and boiled for 5 min in Laemmli sample buffer containing 2.5% β-mercaptoethanol. Electrophoresis was performed using Tris/glycine/SDS running buffer (Boston BioProducts, Inc., Worcester, MA) on 4–20% polyacrylamide gel (Cambrex Bio Science Walkersville, Inc., Walkersville, MD). After transfer to Immun-Blot polyvinylidene difluoride membrane (Bio-Rad), an overnight incubation was performed at 4 °C with anti-gelsolin antibody at a dilution of 1:10,000. Horseradish peroxidase (HRP)-conjugated goat anti-rabbit IgG (Pierce) was then applied at a 1:10,000 dilution for 1 h at room temperature. Proteins were detected using Western Lightning Western Blot Chemiluminescence Reagent Plus (PerkinElmer Life Sciences).

Detection of Proton Secretion Using a Self-referencing Proton-selective Electrode—The effect of actin polymerization by jasplakinolide on proton secretion from intact vas deferens was measured using an extracellular proton-selective electrode as we have described previously (42, 43, 67). The proximal vas deferens was dissected, cut open to expose the apical surface of the epithelium, and bathed in a PBS solution of low buffering capacity (2 mM phosphate). No bath perfusion was performed to allow a proton gradient to build up near the apical surface of V-ATPase-rich cells. The proton-selective electrode was positioned near the surface of the tissue, and oscillations of the electrode were performed perpendicularly to the apical membrane with an amplitude of 50 μm and a frequency of 0.3 Hz. The difference in proton equilibrium potentials, measured at the extreme points of oscillation, is proportional to the proton flux generated by the vas deferens. The Nernstian slope of the electrode was determined before and after each experiment using calibration solutions adjusted to pH 6.0, 7.0, and 8.0. The effect of jasplakinolide was examined on seven vas deferens. A Student's t test for paired experiments was performed, and differences were considered significant at $p < 0.05$. The effect of the vehicle (methanol) was also assessed in a separate group of three vas deferens.

In Vivo Perfusion of the Distal Cauda Epididymidis: V-ATPase Localization and Detection of Endocytosis—Rats were anesthetized as described above. The vas deferens and epididymis were exposed, and the vas deferens was perfused through the lumen using a microcannula (0.4-mm outer diameter, 0.2-mm inner diameter; Kent Scientific, Torrington, CT) as described previously (65). A small incision was made in the distal portion of the cauda epididymidis to allow the perfusate to flow out of the tubule. The vas deferens and distal cauda epididymidis were retrograde-perfused at a rate of 45 μl/min using a syringe pump (Model 100, KD Scientific Inc., Holliston, MA). The lumen was initially washed free of sperm in PBS adjusted to either pH 6.5 or 7.8 (control conditions) as indicated. To detect endocytosis, HRP (Sigma) was added to PBS at a concentration of 5 mg/ml for 15 min. The lumen was then flushed for 3 min with ice-cold PBS adjusted to the appropriate pH to remove non-endocytosed HRP. The vas deferens and cauda epididymidis were harvested and fixed by immersion either for 4 h at room temperature or overnight at 4 °C in PLP fixative. Tissues were washed in PBS and stored in PBS containing 0.02% azide at 4 °C until further utilization.

Some epididymides were subjected to different experimental conditions as described in detail under "Results." To induce actin filament polymerization, 10 μM jasplakinolide (Molecular Probes, Inc., Eugene, Oregon), which binds to F-actin and prevents its depolymerization, was added to the luminal perfusate. To inhibit actin filament assembly, we used a 10-residue peptide derived from the PBD2 PIP_2-binding region of gelsolin (PBP10, 20 μM), provided by Dr. John H. Hartwig (68). This peptide was made membrane-permeable by coupling to rhodamine B and was shown to potentially bind to PIP_2. By competing with gelsolin for binding PIP_2, it prevents the uncapping of gelsolin from F-actin and the gelsolin-dependent desequestering of actin monomers, which are both required for actin assembly (68). Thus, the net effect induced by the PBP10 peptide is depolymerization of the actin cytoskeleton. In addition, to reduce the intracellular calcium concentration, BAPTA-AM (5 μM; Sigma) was added to the luminal perfusate in the absence or presence of the permeant cAMP analog 8-(4-chlorophenylthio)-cAMP (CPT-cAMP; 1 mM; Sigma). Finally, the inhibitor U-73122 (10 μM; Sigma) was used to inhibit PLC.

V-ATPase and HRP internalization was detected by immunofluorescence (65). 5-μm cryostat sections were processed as described above, but an additional permeabilization procedure with 0.1% Triton X-100 was included between the hydration and blocking steps to detect HRP in endosomes. After incubation with chicken anti-V-ATPase antibody and then donkey anti-chicken IgG coupled to fluorescein isothiocyanate, the sections were incubated with anti-HRP polyclonal antibody (Jackson ImmunoResearch Laboratories, Inc.) at a 1:5000 dilution, followed by Cy3-conjugated goat anti-rabbit IgG.

Quantification of V-ATPase Apical Membrane Accumulation—The level of accumulation of V-ATPase in microvilli was quantified by measuring the area occupied by V-ATPase-labeled microvilli as we have described previously (65). Confocal images were imported into IPLab software as TIFF files, and the segmentation procedure was used to measure the area of V-ATPase-positive microvilli. This value was normalized for the width of the cell at the apical pole. At least three epididymides from different animals were perfused for each condition, and a minimum of 10 cells/tissues were examined for a total of at least 30 cells/condition. Analysis of variance and Student's t test were performed. Differences were considered significant at $p < 0.05$.

Confirmation of Actin Polymerization by Jasplakinolide—Rats were anesthetized, and vas deferens were harvested, cut open, and washed free of sperm. The epithelium was peeled off the surrounding connective and muscle tissues as we have described previously (69) and incubated either with 10 μM jasplakinolide in PBS or with the vehicle alone (PBS/methanol) for 45 min at room temperature. Triton X-100-soluble and -insoluble fractions were prepared based on a previous publication (70). The epithelia from both control and jasplakinolide-treated vas deferens were freeze-thawed three times in 100 μl of PBS containing protease inhibitors (Complete mini, Roche Diagnostics) and then centrifuged at 16,000 $\times$ g for 17 min. The supernatant was kept and designated as the soluble fraction. The pellet was homogenized with 100 μl of PBS containing 1% Triton X-100 and protease inhibitors. This fraction was designated as the insoluble fraction.

Equal volumes of each fraction were subjected to electrophoresis to assess the level of polymerized insoluble actin and monomeric soluble actin. Fractions were resuspended in Laemmli sample buffer and boiled for 5 min in Laemmli sample buffer containing 2.5% β-mercaptoethanol. Electrophoresis was performed as described above. Western blotting was performed using monoclonal antibody raised against chicken gizzard actin (1:2000 dilution), followed by HRP-conjugated goat anti-mouse IgG (1:10,000 dilution; Pierce).

Effect of Jasplakinolide on V-ATPase Expression—The vas deferens and distal cauda epididymidis were perfused *in vivo* as described above with PBS containing either 10 μM jasplakinolide or the vehicle alone (methanol). After a 45-min perfusion period, the vas deferens and cauda epididymidis were harvested and immediately frozen in liquid nitrogen for protein extraction. 20 μg of proteins were subjected to electrophoresis as described above. Western blotting using the affinity-purified anti-chicken anti-V-ATPase antibody at a dilution of 1:500 was performed as described above. As a loading control, the same membranes were blotted with α-tubulin monoclonal antibody (1:20,000 dilution; Chemicon International, Inc.).

RESULTS

High Expression of Gelsolin in Clear Cells of the Epididymis

Gelsolin was localized by immunofluorescence in cryostat sections of PLP-fixed epididymis. High levels of gelsolin were detected in clear cells (Fig. 1*A*, *red*), identified by their V-ATPase expression (*yellow*). In contrast, adjacent principal cells were negative for gelsolin. Higher magnification images show that whereas gelsolin was present throughout the cytoplasm of clear cells, it was very abundant in their apical microvilli (Fig. 1*B*, *green*). Double labeling revealed very strong actin staining in the stereocilia of principal cells, but little or no detectable actin in clear cell microvilli (Fig. 1*B*, *red*), indicating

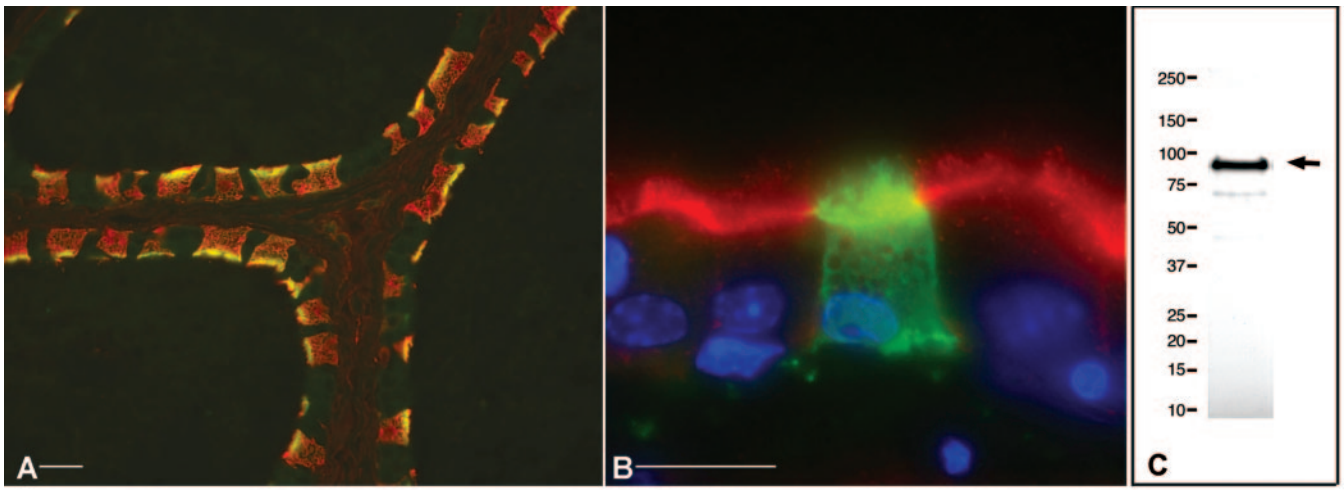

FIG. 1. **Gelsolin localization in the epididymis.** *A*, double immunofluorescence staining showing gelsolin (*red*) and V-ATPase (*yellow*) in rat cauda epididymidis. Strong gelsolin staining was observed in clear cells, identified by their positive immunoreactivity for V-ATPase. Adjacent principal cells were negative for gelsolin. *B*, higher magnification showing gelsolin (*green*) and actin (*red*). Nuclei were stained *blue* by 4′,6-diamidino-2-phenylindole. Although very strong actin staining was detected in the stereocilia of principal cells, no detectable actin was observed in the apical microvilli of clear cells. In these cells, gelsolin was detected throughout the cytoplasm as well as in the apical microvilli. *C*, detection of gelsolin by Western blotting in total homogenates from rat epididymis. 20 μg of protein were loaded onto the gel. A strong band at ~90 kDa was detected, indicating high levels of gelsolin in the epididymis (*arrow*). *Bars* = 25 μm (*A*) and 10 μm (*B*).

that the actin cytoskeleton is much less organized in the apical pole of clear cells compared with principal cells. We postulated that the low level of actin polymerization in clear cells is attributed to their very high gelsolin content. A strong band at ~90 kDa corresponding to gelsolin (71) was detected by Western blotting (Fig. 1*C*).

Effect of Jasplakinolide on Net Proton Secretion

To evaluate the functional role of gelsolin in modulating V-ATPase-dependent proton secretion, we first used the potent actin polymerizing agent jasplakinolide to overcome its action. The effect of jasplakinolide on net proton secretion was examined in cut-open vas deferens using an extracellular proton-selective electrode. As shown in Fig. 2*A* (*upper trace*) and as we have described previously (42, 43, 67), stable proton secretion was detected under control conditions. Addition of the vehicle (methanol) to the control solution induced a transient disturbance of the proton gradient, which rapidly recovered to the control value. Bafilomycin A_1 (1 μM) or concanamycin A (1 μM) induced a rapid decrease in proton secretion, indicating the participation of the V-ATPase. Addition of 10 μM jasplakinolide (Fig. 2*A*, *lower trace*) induced a progressive inhibition of proton secretion compared with the control. At the end of the experimental period, addition of bafilomycin A_1 or concanamycin A had either no or little effect on net proton secretion, indicating a significant reduction in V-ATPase-dependent proton flux by jasplakinolide. Fig. 2*B* shows a histogram of the mean values obtained from a series of seven vas deferens. For each vas deferens, both the control value (measured prior to addition of jasplakinolide) and the jasplakinolide value (measured 40 min after its addition) were corrected for the residual value measured after addition of bafilomycin and/or concanamycin to determine the effect of jasplakinolide on V-ATPase-dependent proton secretion. A Student's *t* test for paired experiments revealed a significant reduction in V-ATPase-dependent proton secretion by jasplakinolide.

Effect of Jasplakinolide on V-ATPase Localization

The effect of jasplakinolide on the localization of V-ATPase and level of endocytosis in clear cells was then examined. In these cells, an increase in V-ATPase surface expression and in apical surface area (including microvilli) closely correlates with an increase in proton secretion. We have shown previously that the V-ATPase relocalizes from intracellular subapical vesicles to the apical microvilli of clear cells in response to an elevation in luminal pH (65). This increase in cell-surface expression of the V-ATPase leads to an increase in the number and length of V-ATPase-labeled microvilli. Here, we tested the effect of jasplakinolide on this alkaline pH-induced response. Epididymides were perfused for 10 min with PBS adjusted to either pH 6.5 or 7.8 and containing 10 μM jasplakinolide or the vehicle alone (methanol). HRP was then added, still in the presence of jasplakinolide or methanol, for an additional period of 15 min. Non-internalized HRP was washed in ice-cold PBS (with or without jasplakinolide) at the appropriate pH for 3 min prior to fixation of the tissue with PLP fixative. As we have described previously (65), under control conditions, clear cells possessed a much higher endocytic activity compared with adjacent principal cells at both acidic and alkaline luminal pH (Fig. 3, *A* and *B*). Under control conditions (methanol) at a luminal pH of 6.5, the V-ATPase was distributed between apical microvilli and intracellular subapical vesicles (Fig. 3*A*). In these cells, V-ATPase-containing vesicles partially co-localized with HRP-containing endosomes (*yellow*), indicating that a significant amount of V-ATPase was located in the endocytic compartment. At an alkaline pH of 7.8, the V-ATPase was located mainly in well developed apical microvilli and was not present in most HRP-positive endosomes, indicating accumulation of V-ATPase in the apical membrane of clear cells (Fig. 3*B*). In contrast, after perfusion in the presence of jasplakinolide at pH 7.8, a complete internalization of V-ATPase was observed, despite the alkaline pH (Fig. 3*C*), leading to the retraction of apical microvilli. Thus, jasplakinolide completely inhibited the alkaline pH-induced V-ATPase apical translocation. A similar V-ATPase internalization was also observed by jasplakinolide at pH 6.5 (data not shown). In addition, no HRP-containing endosomes, either stained or unstained for V-ATPase, were observed under these conditions, indicating that both V-ATPase-related endocytosis and V-ATPase-unrelated endocytosis were inhibited following preincubation with jasplakinolide.

The level of V-ATPase internalization induced by jasplakinolide at alkaline pH was quantified. The intensity of V-ATPase staining in the apical pole of clear cells was measured after

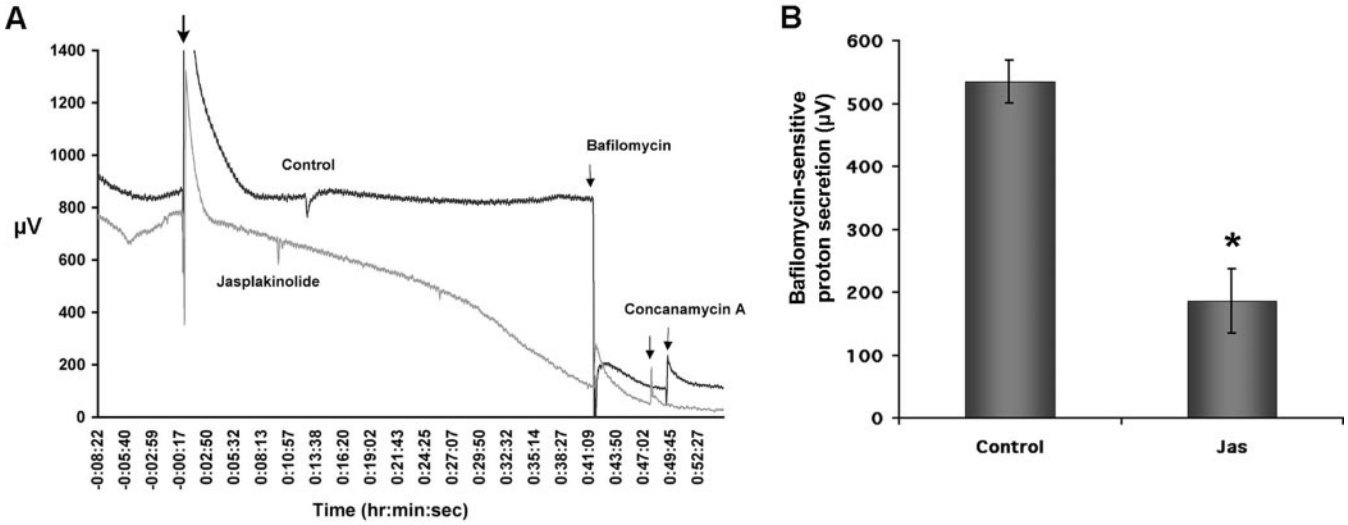

FIG. 2. **Effect of jasplakinolide on proton secretion.** *A*, representative traces showing net proton secretion in cut-open proximal vas deferens under control conditions (*upper trace*) and upon jasplakinolide addition (*lower trace*). Apical proton flux was detected using an extracellular self-referencing proton-selective electrode. *Upper trace*, at time 0, addition of the vehicle (methanol; *arrow*) induced a rapid increase in the signal due to transient disturbance of the proton gradient. The signal then rapidly recovered to the control value as the proton gradient was re-established and remained stable for periods of up to 1 h. A marked inhibition of net proton secretion was observed when bafilomycin A_1 or concanamycin A was added at the end of the experimental period, indicating the participation of V-ATPase in this process. Concanamycin A had no further effect after inhibition by bafilomycin. *Lower trace*, jasplakinolide induced a progressive inhibition of proton secretion to a level that was not further inhibited by bafilomycin A_1 or concanamycin A. *B*, histogram showing the mean effect of jasplakinolide (*Jas*) on bafilomycin-sensitive proton secretion (mean ± S.E., $n = 7$) measured 40 min after addition of jasplakinolide. The control value was measured in the same vas deferens prior to addition of jasplakinolide. Both control and jasplakinolide values were corrected for the residual value measured after bafilomycin A_1 addition. *, $p < 0.001$.

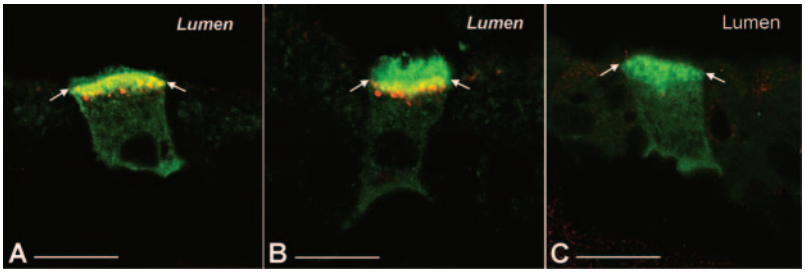

FIG. 3. **Effect of jasplakinolide on pH-induced V-ATPase apical accumulation.** Confocal images showing clear cells from cauda epididymides perfused at a luminal pH of 6.5 (*A*) or 7.8 (*B*) or in the presence of jasplakinolide at pH 7.8 (*C*). Double immunofluorescence labeling for V-ATPase (*green*) and internalized HRP (*red*) was performed. *A*, at a luminal pH of 6.5, a high apical endocytic activity was observed in clear cells compared with principal cells (*yellow* and *red*). In clear cells, V-ATPase was distributed between subapical vesicles and short apical microvilli. The *yellow* staining indicates partial co-localization of HRP-containing endosomes with V-ATPase-containing vesicles. *B*, at a luminal pH of 7.8, a higher apical endocytic activity was also seen in clear cells compared with principal cells, but V-ATPase was located mainly in apical microvilli (*green*) and not in HRP-containing endosomes (*red*). Longer and more numerous microvilli were detected at pH 7.8 compared with pH 6.5. *C*, perfusion with jasplakinolide for a total period of 25 min induced a complete internalization of V-ATPase, despite an alkaline pH of 7.8. A complete retraction of apical microvilli was observed, and no HRP-containing endosomes were detected. The *arrows* indicate the frontier between apical microvilli and the subapical region of clear cells. In *C*, no microvilli were detected. *Bars* = 10 µm.

jasplakinolide treatment using IPLab Spectrum densitometric software. Cryostat sections of control and jasplakinolide-treated epididymides were stained simultaneously for the V-ATPase, and digital images were acquired with identical camera parameters. Lower magnification images were taken to increase the number of cells examined (Fig. 4). Under control conditions, bright V-ATPase staining was observed in the apical pole of clear cells (Fig. 4*A*, *arrows*), whereas in the presence of jasplakinolide, V-ATPase apical staining was significantly reduced (Fig. 4*B*, *arrows*). The mean pixel intensity of the V-ATPase-associated staining in the apical pole of clear cells was quantified using the IPLab Spectrum segmentation procedure as we have described previously (72). A total of 713 and 495 cells were examined from three epididymides exposed to control and jasplakinolide conditions, respectively. As shown in Fig. 4*C*, a significant reduction in V-ATPase apical staining was observed after jasplakinolide treatment. These data suggested either a reduction in V-ATPase expression or redistribution of the V-ATPase throughout the cell following jasplakinolide exposure. Similar levels of V-ATPase protein were detected by Western blotting in epididymides exposed to control and jasplakinolide conditions (Fig. 4*D*, *upper panel*), indicating that jasplakinolide did not affect the expression of V-ATPase. α-Tubulin was used as a loading control in all samples tested (Fig. 4*D*, *lower panel*). Thus, the reduction in V-ATPase apical immunostaining detected in the presence of jasplakinolide is consistent with a reduction in the amount of V-ATPase present in apical microvilli and its redistribution in intracellular vesicles scattered within deeper intracellular regions.

Actin Polymerization by Jasplakinolide

The level of actin polymerization induced by jasplakinolide was tested in epithelial sheets isolated from cut-open vas deferens, a preparation that we have described previously (69). After incubation either in PBS, pH 7.4, or in PBS containing 10 µM jasplakinolide for 45 min, Triton X-100-soluble and -insol-

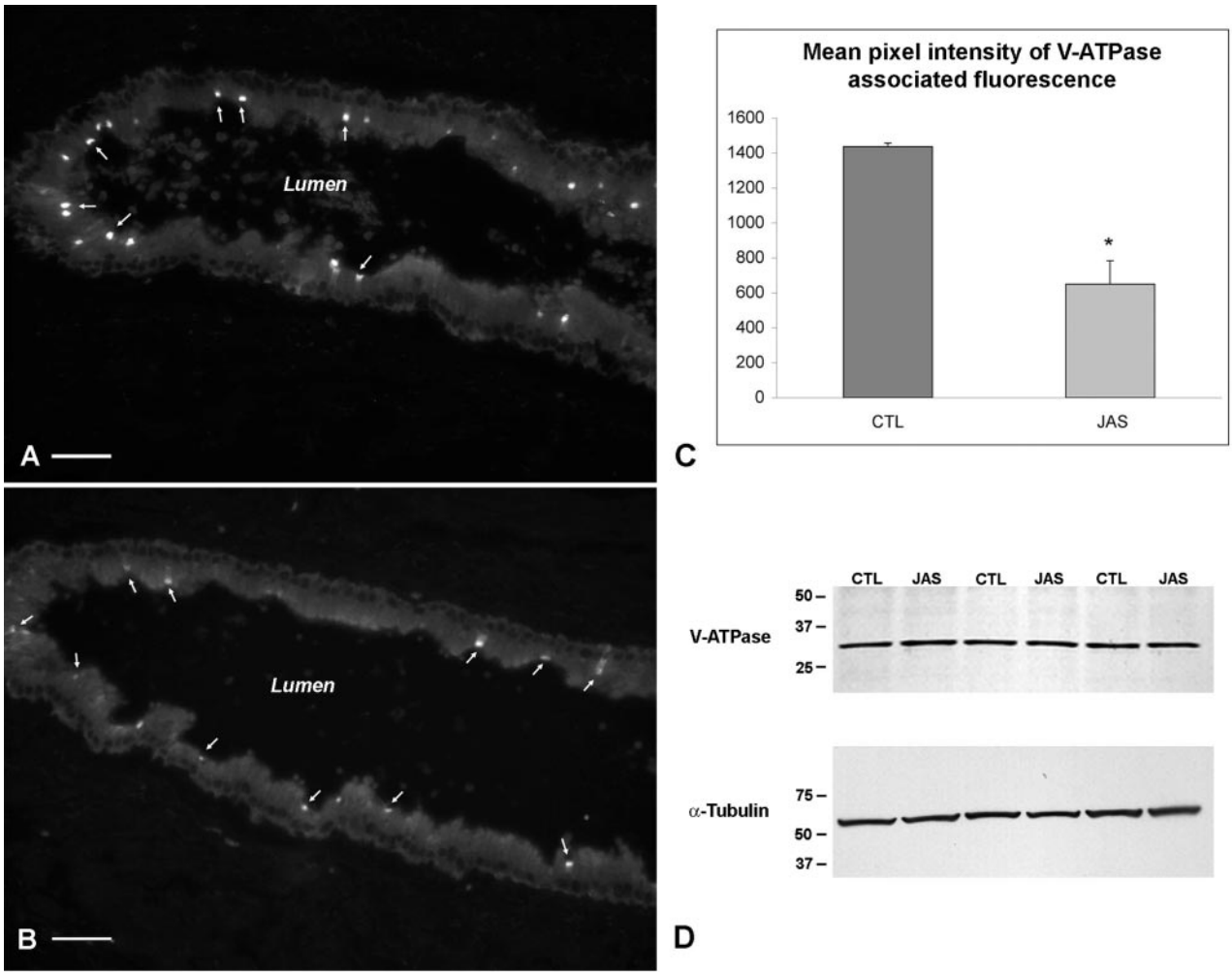

FIG. 4. **Quantification of the effect of jasplakinolide on V-ATPase localization.** Immunofluorescence staining for V-ATPase was performed on cauda epididymides perfused in the absence (*A*) and presence (*B*) of jasplakinolide, and digital images were captured using identical acquisition parameters. *A*: in the absence of jasplakinolide, bright V-ATPase staining was observed in the apical pole of clear cells (*arrows*). *B*: weaker V-ATPase apical staining was detected after jasplakinolide treatment (*arrows*). *C*: the mean pixel intensity of V-ATPase-associated labeling in the apical pole of clear cells was measured using IPLab Spectrum software. A significant decrease in the intensity of V-ATPase staining was observed after jasplakinolide treatment (*JAS*; $n = 495$ cells) compared with the control (*CTL*; $n = 713$ cells). *, $p < 0.005$. *D*: *upper panel*, shown are the results from Western blot analysis of V-ATPase expression in three different epididymides perfused *in vivo* with PBS (control (*CTL*)) or with PBS containing jasplakinolide (*JAS*). 20 μg of total proteins were loaded onto each lane. Western blotting using an antibody against the E subunit (31 kDa) of the V-ATPase revealed similar band intensity in all samples, indicating that jasplakinolide did not affect the total amount of V-ATPase. *Lower panel:* shown are the loading controls using anti-α-tubulin antibody. Similar levels were observed, indicating that the same amount of material was loaded onto each lane.

uble fractions were isolated, and the level of actin was assessed in each fraction by Western blotting. Jasplakinolide induced a marked increase in the amount of insoluble F-actin and a decrease in soluble monomeric actin (G-actin) compared with the control (Fig. 5*A*). Quantification analysis revealed a substantial increase in the ratio between F-actin and G-actin after jasplakinolide treatment compared with the ratio measured under control conditions (Fig. 5*B*), confirming the expected actin polymerization by jasplakinolide. Similar results were obtained in three different experiments.

Effect of Jasplakinolide on cAMP-induced Apical Accumulation of V-ATPase

We have shown previously that cAMP induces the accumulation of V-ATPase in apical microvilli, even at acidic luminal pH (65). We tested whether this process is affected by jasplakinolide. Epididymides were perfused for 10 min with jasplakinolide, followed by a 15-min perfusion with the permeant cAMP analog CPT-cAMP (1 mM), still in the presence of jasplakinolide. We first examined the localization of V-ATPase after the first 10 min of jasplakinolide exposure. As shown in Fig. 6*A*, V-ATPase was located mainly in apical vesicles, and very few short V-ATPase-labeled microvilli were detected under these conditions, indicating that the majority of V-ATPase internalization took place during the first 10 min of jasplakinolide exposure. Addition of CPT-cAMP after this preincubation period for a period of 15 min did not cause significant apical accumulation of V-ATPase (Fig. 6*B*), and almost no V-ATPase-labeled microvilli were detected. Control epididymides were perfused for a period of 15 min with CPT-cAMP without jasplakinolide. Consistent with our previously published data (65), V-ATPase was present mostly in well developed apical microvilli (Fig. 6*C*), indicating apical redistribution of V-ATPase by cAMP. These results indicate that jasplakinolide inhibited the cAMP-induced V-ATPase accumulation in apical microvilli.

We postulated that the maintenance of a depolymerized actin cytoskeleton, possibly via gelsolin activity, is essential for the recycling of V-ATPase. To test this hypothesis, a PIP_2-binding peptide (PBP10) that corresponds to the PDB2 PIP_2-

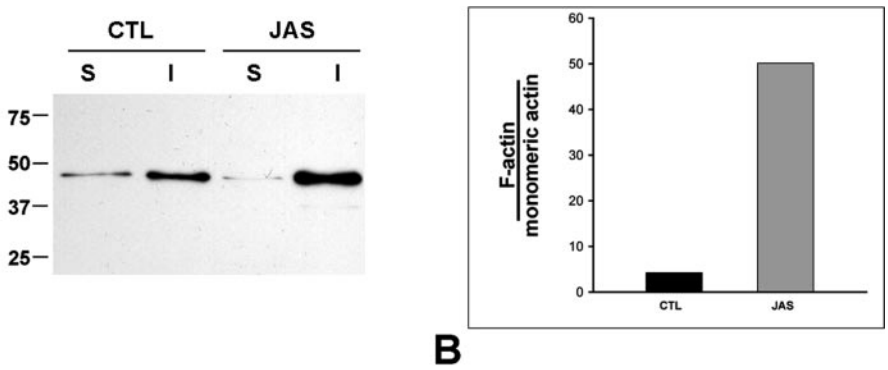

FIG. 5. **Actin polymerization by jasplakinolide.** *A*, shown are the results from Western blot analysis of the amount of actin present in the Triton X-100-soluble (*S*) and -insoluble (*I*) fractions of epithelial cell sheets isolated from proximal vas deferens incubated with PBS (control (*CTL*)) or jasplakinolide (*JAS*) for 45 min. Both soluble and insoluble fractions were solubilized in SDS-containing sample buffer, and an equal volume of each fraction was loaded onto the gel. Western blotting using anti-actin antibody revealed that the amount of soluble monomeric G-actin was markedly reduced and that the amount of insoluble F-actin was increased after jasplakinolide treatment. *B*, semiquantitative analysis of the intensity of the bands revealed, as expected, that jasplakinolide induced a marked increase in the ratio of insoluble to soluble fractions compared with the control, indicating significant polymerization of the actin cytoskeleton.

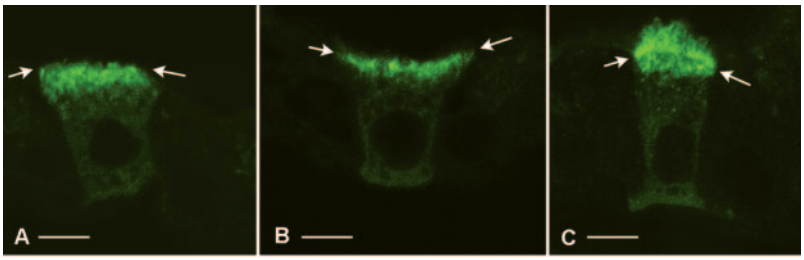

FIG. 6. **Effect of jasplakinolide on cAMP-induced V-ATPase apical accumulation.** The confocal images show clear cells from cauda epididymides perfused with PBS containing jasplakinolide for 10 min (*A*); with PBS containing jasplakinolide for 10 min, followed by CPT-cAMP, still in the presence of jasplakinolide for 15 min (*B*); or with PBS containing CPT-cAMP for 15 min (*C*). *A*, V-ATPase was present in apical vesicles, and no apical microvilli were detected, indicating significant V-ATPase internalization. *B*, no apical microvilli were detected, and V-ATPase was located mainly in subapical vesicles, despite the presence of CPT-cAMP, indicating that preincubation with jasplakinolide abolished the cAMP-induced V-ATPase apical translocation. *C*, the majority of V-ATPase was located in well developed apical microvilli, indicating that cAMP induced the usual apical translocation of the pump. V-ATPase-labeled subapical vesicles were also detected. The *arrows* indicate the frontier between the apical cytoplasm and the base of the apical microvilli. In *A* and *B*, no apical microvilli were detected. *Bars* = 5 μm.

binding region of gelsolin (68) was used. This peptide prevents the binding of PIP_2 to gelsolin.

Effect of the PIP_2-binding Peptide PBP10 on V-ATPase Recycling

As mentioned above, PIP_2 binds to gelsolin and dissociates it from the barbed ends of actin filaments, thus promoting actin polymerization. By preventing the binding of PIP_2 to gelsolin, the PBP10 peptide favors the establishment of a depolymerized actin cytoskeleton (68). The effect of PBP10 on the distribution of V-ATPase in epididymides perfused at either acidic or alkaline luminal pH was tested. The epididymides were first perfused with PBS with or without PBP10 (20 μM) for 10 min. Horseradish peroxidase was then added for an additional period of 15 min, and washes were performed as described above. In the presence of PBP10 at a luminal pH of 6.5, the V-ATPase was located mainly in apical microvilli, and very little or no co-localization with HRP-containing endosomes was detected (Fig. 7*A*), a situation that resembled the V-ATPase localization observed under control conditions at alkaline pH (compare with Fig. 3*B*). Thus, PBP10 induced the apical accumulation of V-ATPase, despite the acidic luminal pH. At a luminal pH of 7.8, the usual microvillus localization of V-ATPase was observed in the presence of the peptide (Fig. 7*B*). The level of insertion of V-ATPase into microvilli was quantified using IPLab Spectrum software as we have described previously (65). We have shown, by immunoelectron microscopy, that the apical microvillus extension observed at alkaline pH is accompanied by an increase in the number of V-ATPase molecules associated with the plasma membrane, indicating that accumulation of V-ATPase in the membrane occurs in parallel with the development of apical microvilli (65). Thus, the area occupied by V-ATPase-labeled microvilli was measured and normalized for the width of the cells at the apical pole for each cell and was used as an indicator of the level of V-ATPase accumulation in apical microvilli as we have described previously (65). As shown in Fig. 8, the surface occupied by the apical microvilli was significantly increased in the presence of PBP10 at a luminal pH of 6.5 (*PBP10 6.5*) compared with the control (*CTL 6.5*) and was not different from that measured under control conditions at a luminal pH of 7.8 (*CTL 7.8*). No additional effect of the peptide was observed at pH 7.8 (*PBP10 7.8*) compared with the control (*CTL 7.8*). These results indicate that the PBP10 peptide induced the apical accumulation of V-ATPase at acidic luminal pH, but had no significant effect on V-ATPase localization at alkaline pH.

Role of Calcium in Regulating V-ATPase Recycling

In addition to its role in modulating the actin cytoskeleton, gelsolin has also been proposed to participate in intracellular calcium signaling by controlling the availability of PIP_2 substrates (73). Inhibition of PLC following competition with gelsolin for PIP_2 was shown both *in vivo* and *in vitro* (73, 74). As calcium is actively involved in the regulation of vesicle recycling and in modulating V-ATPase-dependent proton secretion in some acidifying cells (75, 76), we examined whether the effects observed with the PBP10 peptide might be attributed to alteration of the calcium signaling pathway.

Effect of BAPTA-AM on pH-regulated V-ATPase Recycling—First, the effect of the calcium chelator BAPTA-AM on V-

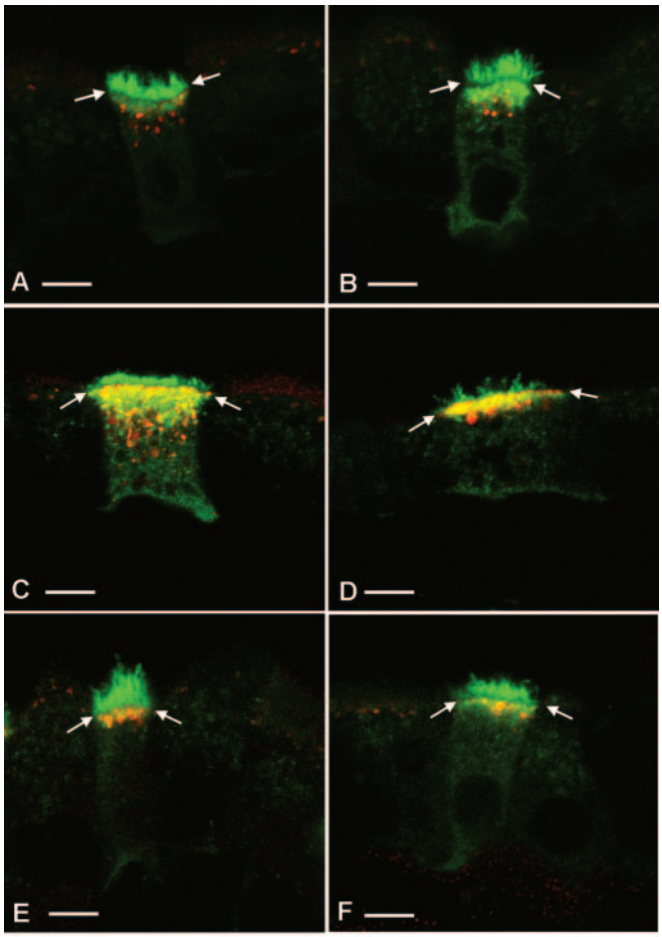

FIG. 7. **Role of gelsolin and calcium in pH- and cAMP-dependent V-ATPase recycling.** The confocal images show clear cells exposed to different luminal conditions and double-stained for V-ATPase (*green*) and HRP (*red*). *A* and *B*, perfusion with PBS containing PBP10 (a peptide that corresponds to the PBD2 PIP_2-binding site of gelsolin) at pH 6.5 and 7.8, respectively. *A*, at pH 6.5, V-ATPase was located mainly in well developed apical microvilli. No *yellow* staining was visible, indicating the absence of co-localization with HRP-containing endosomes. This result indicates that PBP10 induced V-ATPase apical accumulation, despite the acidic luminal pH. *B*, at pH 7.8, V-ATPase was also located mainly in apical microvilli, and little or no co-localization was observed in HRP-labeled endosomes. *C* and *D*, PBS containing BAPTA-AM at pH 6.5 and 7.8, respectively. *C*, at pH 6.5, high levels of V-ATPase-related (*yellow*) and V-ATPase-unrelated (*red*) endocytosis were observed. The apical microvillus number and length were similar to those seen under control conditions at this pH (compare with Fig. 3*A*). *D*, at pH 7.8, V-ATPase was distributed between apical microvilli and HRP-containing endosomes (*yellow*). The apical microvilli were less numerous and shorter compared with the controls at this pH (compare with Fig. 3*B*). *E* and *F*, PBS containing CPT-cAMP at pH 6.5 in the absence and presence of BAPTA-AM, respectively. *E*, CPT-cAMP induced the accumulation of V-ATPase in well developed microvilli. This result is similar to that shown in Fig. 6*C*. *F*, Shorter V-ATPase-labeled microvilli were seen when CPT-cAMP was added in the presence of BAPTA-AM. The *arrows* point to the frontier between apical microvilli and the subapical region of the cells. *Bars* = 5 μm.

ATPase recycling was examined at acidic and alkaline luminal pH. Epididymides were perfused with PBS, pH 6.5 or 7.8, containing 5 μM BAPTA-AM for 10 min, followed by PBS containing HRP and BAPTA-AM for 15 min. Washes were performed in the presence of BAPTA-AM. At pH 6.5, BAPTA-AM increased the level of both V-ATPase-related (Fig. 7*C*, *yellow*) and V-ATPase-unrelated (*red*) endocytosis. At pH 7.8, BAPTA-AM prevented the accumulation of V-ATPase in apical microvilli (Fig. 7*D*) and induced some degree of V-ATPase internalization (*yellow*). Quantification analysis confirmed that chelation of calcium with BAPTA induced a marked decrease in the surface occupied by V-ATPase-positive microvilli at pH 7.8 (Fig. 8, *BAPTA 7.8*) compared with the control (*CTL 7.8*). No effect of BAPTA-AM was detected at pH 6.5 (Fig. 8, *BAPTA 6.5 versus CTL 6.5*).

Effect of BAPTA-AM on cAMP-induced Apical Accumulation of V-ATPase—We have shown previously that apical membrane accumulation of the V-ATPase is triggered by a soluble adenylyl cyclase (sAC)-dependent elevation in cAMP in response to alkaline luminal pH (65). As sAC is regulated by calcium (77), we tested whether the inhibition of the alkaline pH-induced V-ATPase accumulation that we observed in the presence of BAPTA-AM might have been secondary to reduced activity of this enzyme. The effect of the permeant cAMP analog CPT-cAMP was measured in the presence of BAPTA-AM (Fig. 7*F*). Epididymides were perfused at a luminal pH of 6.5 with PBS containing BAPTA-AM (5 μM) for 10 min, followed by PBS containing BAPTA-AM, HRP, and 1 mM CPT-cAMP for 15 min. Washes were performed with cold PBS containing BAPTA-AM and cAMP. The same protocol was repeated in the absence of BAPTA-AM. Consistent with our previous study (65), in the absence of BAPTA-AM, very well developed V-ATPase-positive apical microvilli were detected with CPT-cAMP (Fig. 7*E*). This result is similar to that shown in Fig. 6*C*. Quantification analysis revealed that CPT-cAMP induced a significant increase in the area occupied by V-ATPase-positive microvilli compared with the control pH 6.5 group (Fig. 8, *CTL 6.5 + cAMP versus CTL 6.5*), indicating apical membrane accumulation of the V-ATPase, despite the acidic luminal pH. In contrast, shorter V-ATPase-positive microvilli were observed when CPT-cAMP was added after preincubation with BAPTA-AM (Fig. 7*F*) compared with the control CPT-cAMP group (Fig. 7*E*). Quantification analysis revealed a significant inhibition of the cAMP-induced V-ATPase apical accumulation by BAPTA-AM (Fig. 8, *BAPTA 6.5 + cAMP versus CTL 6.5 + cAMP*). This result indicates that intracellular calcium is a key player in the cAMP-induced response and that the effects of BAPTA-AM occurred downstream of sAC activity.

Role of PLC in pH-regulated V-ATPase Recycling—Finally, we tested whether the PIP_2-dependent PLC pathway is involved in V-ATPase recycling. Epididymides were perfused at pH 6.5 and 7.8 with the PLC inhibitor U-73122 (10 μM) or with the vehicle alone (Me_2SO) for 30 min prior to adding HRP for 15 min, still in the presence of U-73122 or Me_2SO alone. The epididymides were then processed as described above. Whereas no effect of U-73122 was observed at pH 6.5 (Fig. 9, *A* and *C*, *U-73122 6.5*) compared with the control (Fig. 9*C*, *CTL 6.5*), a significant reduction in the area occupied by V-ATPase-positive apical microvilli was observed at pH 7.8 (Fig. 9, *B* and *C*, *U-73122 7.8*) compared with the control (Fig. 9*C*, *CTL 7.8*).

These results indicate that the alkaline pH-induced apical insertion of the V-ATPase depends on the PLC-dependent calcium signaling pathway. They also show that the stimulatory effects induced by the PBP10 peptide were not due to impairment of the PIP_2-dependent PLC pathway since inhibition of PLC resulted in the opposite effect.

DISCUSSION

This study shows that clear cells of the epididymis express very high levels of gelsolin, a common feature of other specialized V-ATPase-expressing proton-secreting cells: kidney intercalated cells and osteoclasts. We examined whether modulation of the actin cytoskeleton via gelsolin might play a role in regulating V-ATPase recycling. We have shown previously that V-ATPase accumulates in the apical microvilli of clear cells in response to an elevation in luminal pH (65), a process that would increase proton secretion and re-establish the resting acidic luminal pH of the epididymis, which is

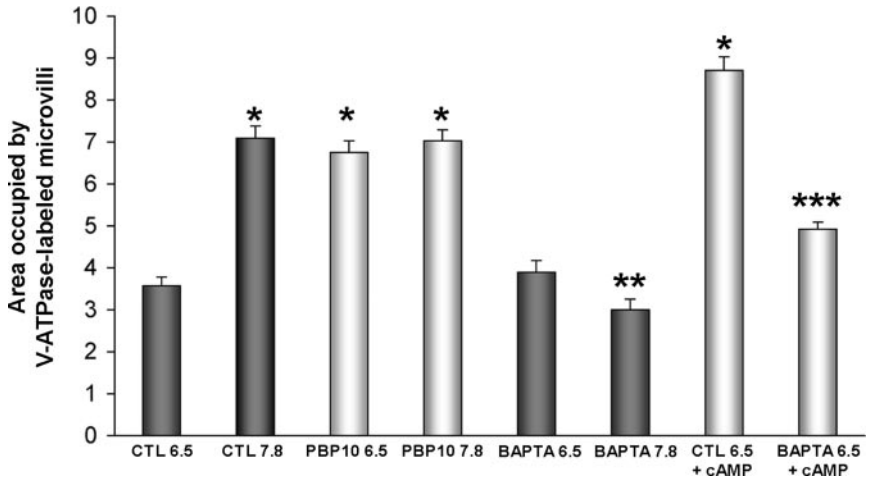

FIG. 8. **Quantification of V-ATPase accumulation in apical microvilli.** The level of V-ATPase accumulation in microvilli was quantified by measuring the area occupied by V-ATPase-labeled microvilli, normalized for the width of the cells at the apical pole for each cell. Control groups were epididymides perfused with PBS containing the vehicle (Me_2SO) for 10 min, followed by HRP for 15 min in PBS containing Me_2SO at a luminal pH of 6.5 or 7.8. Under control conditions, the area occupied by V-ATPase-positive microvilli was significantly higher at a luminal pH of 7.8 (*CTL 7.8*) compared with a luminal pH of 6.5 (*CTL 6.5*). The PBP10 peptide induced a significant increase at pH 6.5 (*PBP10 6.5*) compared with the control (*CTL 6.5*). No effect was induced by PBP10 at pH 7.8 (*PBP10 7.8*) compared with the control (*CTL 7.8*). BAPTA-AM prevented the increase in the area occupied by V-ATPase-positive microvilli induced at pH 7.8 (*BAPTA 7.8 versus CTL 7.8*), but had no effect on the microvillus area observed at pH 6.5 (*BAPTA 6.5 versus CTL 6.5*). In the absence of BAPTA-AM, CPT-cAMP induced a significant increase in the area occupied by V-ATPase microvilli, despite the acidic pH of 6.5 (*CTL 6.5 + cAMP versus CTL 6.5*). In contrast, BAPTA-AM markedly decreased the response induced by CPT-cAMP (*BAPTA 6.5 + cAMP versus CTL 6.5 + cAMP*). *, $p < 0.05$ *versus CTL 6.5*; **, $p < 0.05$ *versus CTL 7.8*; ***, $p < 0.05$ *versus CTL 6.5 + cAMP*.

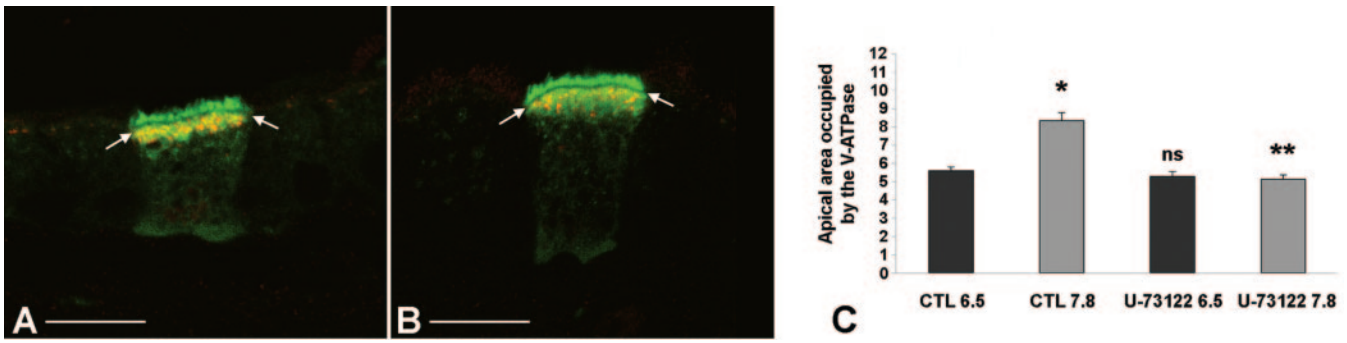

FIG. 9. **Effect of the PLC inhibitor U-73122 on pH-regulated V-ATPase recycling.** Cauda epididymides were perfused with PBS adjusted to pH 6.5 (*A*) or 7.8 (*B*) and containing U-73122 for 30 min, followed by a 15-min perfusion with HRP, still in the presence of U-73122. Controls were carried out with a pre-perfusion period of 30 min with PBS containing the vehicle (Me_2SO) at both pH values, followed by 15 min with PBS containing HRP and Me_2SO. Double immunofluorescence labeling for V-ATPase (*green*) and HRP (*red*) was performed. *A*, at pH 6.5 in the presence of U-73122, V-ATPase was distributed between short apical microvilli and subapical HRP-containing vesicles, as for the control at pH 6.5 (compare with Fig. 3*A*). *B*, at pH 7.8, U-73122 prevented the elongation of microvilli that was usually seen under control conditions (compare with Fig. 3*B*), and V-ATPase was distributed between intracellular endosomes and short apical microvilli. *C*, quantification of the area occupied by V-ATPase-labeled microvilli confirmed that inhibition of PLC by U-73122 prevented the alkaline-pH induced accumulation of V-ATPase in apical microvilli (*U-73122 7.8 versus CTL 7.8*). Identical microvillus area values were measured in the presence or absence of U-73122 at pH 6.5 (*U-73122 6.5 versus CTL 6.5*). *, $p < 0.05$ *versus CTL 6.5*; **, $p < 0.05$ *versus CTL 7.8*; *ns*, not significantly different *versus CTL 6.5*. *Bars* = 10 μm.

necessary for sperm maturation and storage. A concomitant significant increase in the number and length of apical microvilli, which contained a higher number of V-ATPase molecules/unit length of membrane, was observed under these conditions. At acidic luminal pH, the V-ATPase constitutively recycles, and a major portion of the pump is present in HRP-labeled endosomes. Both the alkaline pH-induced membrane accumulation and acidic pH-dependent internalization of the V-ATPase occur rapidly, within 15 min. An elevation in cAMP via sAC participates in the pH-induced V-ATPase apical accumulation (65). Thus, alkalinization of luminal pH, followed by an increase in intracellular pH in clear cells, leads to 1) elevation of the intracellular bicarbonate concentration, 2) activation of sAC by bicarbonate, 3) elevation of cAMP, and 4) accumulation of V-ATPase in apical microvilli (65).

In this study, we hypothesized that the high level of gelsolin in clear cells would favor V-ATPase apical accumulation, in response to luminal pH elevation and/or cAMP increase, by maintaining the actin cytoskeleton in a depolymerized state. To test this hypothesis, we used the potent polymerizing agent jasplakinolide to overcome the action of gelsolin. The complete inhibition of alkaline pH- or cAMP-induced V-ATPase apical accumulation by jasplakinolide indicates that dynamic remodeling of the actin cytoskeleton is required for these processes to occur. In addition, a permeant peptide (PBP10) that mimics the PBD2 PIP_2-binding site of gelsolin (68) induced a significant accumulation of V-ATPase in apical microvilli at acidic luminal pH. PBP10 blocks actin assembly by preventing the uncapping of gelsolin from the growing ends of the actin filaments and induces major disruption of the actin cytoskeleton (68). A recent study has shown that, in osteoclasts, peptides containing the phosphoinositide-binding domains of gelsolin inhibit the dissociation of endogenous gelsolin from actin filaments (41). This results in loss of the actin ring located at the periphery of the cells and prevents osteopontin-induced actin polymeriza-

tion. Thus, in this study, we propose that the apical accumulation of V-ATPase generated by the PBP10 peptide at acidic pH was secondary to the induction of a less polymerized actin cytoskeleton. No additional effect of PBP10 was observed on V-ATPase distribution at a luminal pH of 7.8, suggesting that the actin cytoskeleton was already maintained in a more depolymerized state via gelsolin at alkaline pH. These results indicate a major role for gelsolin in modulating the intracellular and plasma membrane distribution of V-ATPase.

Because PBP10 might also have affected other PIP_2-related events within the cells, especially the highly PIP_2-dependent PLC calcium signaling pathway (73), we examined the potential involvement of calcium and PLC in V-ATPase recycling. Both chelation of calcium with BAPTA-AM and inhibition of PLC by U-73122 significantly inhibited the apical accumulation of V-ATPase induced by alkaline luminal pH. These results indicate the requirement of the PLC calcium signaling pathway in this process. The effect of BAPTA-AM occurred downstream of sAC since inhibition of V-ATPase accumulation was also observed when BAPTA-AM was added in the presence of CPT-cAMP. This ruled out the possibility that the effect of BAPTA-AM on V-ATPase distribution was secondary to inhibition of sAC, an enzyme that can also be regulated by calcium. Importantly, these data also show that the effect of PBP10 was not due to impairment of the PLC pathway. Indeed, opposite results would have been expected if such an interaction had occurred.

Our data indicate that active remodeling of the actin cytoskeleton by gelsolin plays a key role in V-ATPase recycling. At alkaline luminal pH, maintenance of the actin cytoskeleton in a depolymerized state by gelsolin would facilitate the apical membrane mobilization of V-ATPase via 1) an increase in the rate of V-ATPase exocytosis, 2) a decrease in the rate of V-ATPase endocytosis, or 3) a combination of both processes. At a luminal pH of 6.5, these processes would be reversed to facilitate internalization of the V-ATPase. Very little co-localization of V-ATPase with HRP-labeled endosomes was observed under control conditions at alkaline pH or in the presence of CPT-cAMP (this study and Ref. 65), indicating that reduction of V-ATPase endocytosis is an important event for its apical membrane accumulation. In this respect, the V-ATPase resembles another membrane protein, AQP2, for which inhibition of endocytosis either by depletion of membrane cholesterol (78) or by expression of dominant-negative GTPase-deficient K44A dynamin (79) is sufficient to induce its plasma membrane accumulation. Interestingly, numerous larger HRP-containing endosomes not labeled for V-ATPase were seen at alkaline luminal pH or upon CPT-cAMP exposure (Figs. 3*B* and 7*E*, *red*). We postulated that this V-ATPase-independent endocytic pathway is activated secondary to massive apical membrane accumulation of V-ATPase to prevent an overly excessive increase in the apical surface of the cell. This partially compensatory mechanism was previously proposed for other actively recycling membrane proteins (80). Activation of the V-ATPase-independent endocytic pathway would also contribute to the increase in the number of V-ATPase molecules/unit length of apical membrane that we observed at alkaline pH (65). Interestingly, a decrease in the amount of internalized V-ATPase in HRP-labeled endosomes was observed in epididymides perfused at pH 6.5 with PBP10, whereas numerous V-ATPase-negative endosomes were detected (Fig. 7*A*), a situation similar to that observed under control alkaline pH conditions. This result indicates that whereas the V-ATPase-related endocytic compartment was inhibited by PBP10, V-ATPase-independent endocytosis was still taking place. Thus, depolymerization of the actin cytoskeleton by PBP10 at acidic pH would favor the apical accumulation of V-ATPase in a manner similar to that induced at alkaline pH via inhibition of V-ATPase endocytosis. This points to a specific role for gelsolin in inhibiting V-ATPase endocytosis in response to alkaline pH, whereas V-ATPase-unrelated endocytosis can still occur. Accordingly, a more depolymerized actin cytoskeleton produced by gelsolin action at alkaline luminal pH would favor the apical accumulation of V-ATPase, at least partially via reduction of endocytosis.

In addition, the significant V-ATPase apical accumulation induced by PBP10 at acidic luminal pH, a condition under which clear cells normally do not show maximal V-ATPase surface expression, strongly suggests that depolymerization of the actin cytoskeleton by PBP10 represents a sufficient trigger for this process to occur. Other studies have shown that modulation of the actin cytoskeleton is important for the regulation of AQP2 recycling (27) and that depolymerization of the actin cytoskeleton is sufficient to induce its cell-surface accumulation (25).

Interestingly, a complete redistribution of V-ATPase from apical microvilli to intracellular vesicles was observed after a period of 25 min in the presence of jasplakinolide at both acidic and alkaline luminal pH. A corresponding inhibition of bafilomycin-sensitive net proton secretion was detected under these conditions using the self-referencing proton-selective electrode. These results are compatible with increased endocytosis and/or decreased exocytosis of the V-ATPase. A previous study has shown an increase in basolateral endocytosis, but no effect of jasplakinolide on apical endocytosis in Madin-Darby canine kidney cells (70). In our study, no or very few HRP-labeled endosomes, either stained or negative for V-ATPase, were detected when HRP was added to the luminal perfusate for 15 min after a preincubation period of 10 min with jasplakinolide, at which time most of the actin cytoskeleton was probably in a very polymerized state. We hypothesized that the bulk of V-ATPase internalization occurred during the jasplakinolide preincubation period. This was confirmed by the complete intracellular redistribution of V-ATPase that was observed after a 10-min incubation with jasplakinolide. At this time point, cAMP failed to induce V-ATPase apical accumulation when applied in the continued presence of jasplakinolide. We have shown previously that cAMP can induce the apical membrane re-insertion of V-ATPase that has been internalized following acetazolamide treatment (65), and we proposed that cAMP can stimulate V-ATPase exocytosis. In our present study, since most of the V-ATPase had been internalized by jasplakinolide prior to addition of cAMP, it appears that actin polymerization inhibited the exocytosis of V-ATPase. Thus, complete internalization of V-ATPase by jasplakinolide would result from the initial activation of V-ATPase endocytosis, followed by the progressive inhibition of exocytosis. Similarly, actin polymerization inhibits the exocytosis of amylase-containing vesicles in pancreatic acinar cells (18), and expression of constitutively active RhoA to induce actin polymerization inhibits vasopressin-induced AQP2 membrane accumulation (25).

The mechanisms responsible for the apical membrane accumulation of V-ATPase that occurs in response to alkaline luminal pH or cAMP elevation are still not fully characterized. None of the subunits of the V-ATPase have been shown to be phosphorylated by protein kinase A (49, 50), which indicates that an indirect mechanism might be involved in the cAMP-induced apical accumulation of the pump. Interestingly, modulation of the actin cytoskeleton by cAMP has been proposed for the regulation of several membrane transporters (81–86), and phosphorylation of RhoA by protein kinase A, leading to actin disassembly, was invoked in their regulation. In this study, depolymerization of the actin cytoskeleton by cAMP,

leading to inhibition of V-ATPase endocytosis, would be compatible with the apical accumulation of V-ATPase induced by cAMP. Thus, cAMP would exert its action via both an increase in V-ATPase exocytosis and a decrease in V-ATPase endocytosis. Whether cAMP acts via modulation of the actin cytoskeleton or via an independent pathway or whether both processes take place still remains to be elucidated.

Our results point to a significant role for gelsolin in regulating V-ATPase recycling via modulation of the actin cytoskeleton. The severing activity of gelsolin is strongly dependent on intracellular calcium (37, 87, 88). Although high calcium concentrations were initially reported to be required for gelsolin activation, a conformational switch that reduces considerably the required concentrations of calcium to nanomolar ranges has recently been described in villin (89), a protein homologous to gelsolin (90, 91). It was proposed that both villin and gelsolin are maintained in an autoinhibited conformation and that, upon tyrosine phosphorylation, a conformational modification occurs that reveals high affinity sites for calcium. This model is in agreement with our results showing the absolute requirement of calcium for the alkaline pH-induced accumulation of V-ATPase. To determine whether tyrosine phosphorylation is involved in this process will require further studies. The calcium requirement of gelsolin was shown to depend on pH (92), but the pH necessary to regulate gelsolin *in vitro* is very low (pH <6.0) and is unlikely to be reached intracellularly.

We (59) and others (55–58) have shown that the V-ATPase interacts directly or indirectly with actin. V-ATPase binds to F-actin, but not to G-actin, and in osteoclasts, internalization of V-ATPase is correlated with increased interaction with actin (56). We are currently investigating the possibility that the interaction between V-ATPase and actin can also be modulated in clear cells.

In conclusion, this study shows high expression of gelsolin in clear cells of the epididymis and that modulation of the actin cytoskeleton by gelsolin plays a key role in the regulation of V-ATPase surface expression. As gelsolin is also expressed in other cells expressing the V-ATPase in their plasma membrane, including kidney intercalated cells and osteoclasts, we propose that modulation of the actin cytoskeleton by this severing and capping protein represents a common mechanism by which these cells can regulate their rate of proton secretion.

REFERENCES

1. Mitchison, T. J., and Cramer, L. P. (1996) *Cell* **84,** 371–379
2. Hartwig, J. H., and Kwiatkowski, D. J. (1991) *Curr. Opin. Cell Biol.* **3,** 87–97
3. Lauffenburger, D. A., and Horwitz, A. F. (1996) *Cell* **84,** 359–369
4. Blanchoin, L., Amann, K. J., Higgs, H. N., Marchand, J. B., Kaiser, D. A., and Pollard, T. D. (2000) *Nature* **404,** 1007–1011
5. Machesky, L. M., and Insall, R. H. (1999) *J. Cell Biol.* **146,** 267–272
6. Cunningham, C. C., Stossel, T. P., and Kwiatkowski, D. J. (1991) *Science* **251,** 1233–1236
7. Wong, G. K., Allen, P. G., and Begg, D. A. (1997) *Cell Motil. Cytoskeleton* **36,** 30–42
8. Pavalko, F. M., and Otey, C. A. (1994) *Proc. Soc. Exp. Biol. Med.* **205,** 282–293
9. Bernstein, B. W., DeWit, M., and Bamburg, J. R. (1998) *Mol. Brain Res.* **53,** 236–251
10. Lang, T., Wacker, I., Wunderlich, I., Rohrbach, A., Giese, G., Soldati, T., and Almers, W. (2000) *Biophys. J.* **78,** 2863–2877
11. Kjeken, R., Egeberg, M., Habermann, A., Kuehnel, M., Peyron, P., Floetenmeyer, M., Walther, P., Jahraus, A., Defacque, H., Kuznetsov, S. A., and Griffiths, G. (2004) *Mol. Biol. Cell* **15,** 345–358
12. Hartwig, J. H., Brown, D., Ausiello, D. A., Stossel, T. P., and Orci, L. (1990) *J. Histochem. Cytochem.* **38,** 1145–1153
13. Orci, L., Gabbay, K. H., and Malaisse, W. J. (1972) *Science* **175,** 1128–1130
14. Fath, K. R., Mamajiwalla, S. N., and Burgess, D. R. (1993) *J. Cell Sci. Suppl.* **17,** 65–73
15. Durrbach, A., Louvard, D., and Coudrier, E. (1996) *J. Cell Sci.* **109,** 457–465
16. Riezman, H., Munn, A., Geli, M. I., and Hicke, L. (1996) *Experientia* (*Basel*) **52,** 1033–1041
17. Buss, F., Luzio, J. P., and Kendrick-Jones, J. (2001) *FEBS Lett.* **508,** 295–299
18. Muallem, S., Kwiatkowska, K., Xu, X., and Yin, H. L. (1995) *J. Cell Biol.* **128,** 589–598
19. Brown, D. (2003) *Am. J. Physiol.* **284,** F893–F901
20. Apodaca, G. (2001) *Traffic* **2,** 149–159
21. Hoekstra, D., Tyteca, D., and van IJzendoorn, S. C. (2004) *J. Cell Sci.* **117,** 2183–2192S. C. D.
22. Sontag, J. M., Aunis, D., and Bader, M. F. (1988) *Eur. J. Cell Biol.* **46,** 316–326
23. Morita, K., Oka, M., and Hamano, S. (1988) *Biochem. Pharmacol.* **37,** 3357–3359
24. Brozinick, J. T., Jr., Hawkins, E. D., Strawbridge, A. B., and Elmendorf, J. S. (2004) *J. Biol. Chem.* **279,** 40699–40706
25. Klussmann, E., Tamma, G., Lorenz, D., Wiesner, B., Maric, K., Hofmann, F., Aktories, K., Valenti, G., and Rosenthal, W. (2001) *J. Biol. Chem.* **276,** 20451–20457
26. Ausiello, D. A., Hartwig, J., and Brown, D. (1987) *Soc. Gen. Physiol. Ser.* **42,** 259–275
27. Hays, R. M., Condeelis, J., Gao, Y., Simon, H., Ding, G., and Franki, N. (1993) *Pediatr. Nephrol.* **7,** 672–679
28. Dibas, A., Mia, A., and Yorio, T. (2000) *Proc. Soc. Exp. Biol. Med.* **223,** 203–209
29. Gottlieb, T. A., Ivanov, I. E., Adesnik, M., and Sabatini, D. D. (1993) *J. Cell Biol.* **120,** 695–710
30. Jackman, M. R., Shurety, W., Ellis, J. A., and Luzio, J. P. (1994) *J. Cell Sci.* **107,** 2547–2556
31. Fujimoto, L. M., Roth, R., Heuser, J. E., and Schmid, S. L. (2000) *Traffic* **1,** 161–171
32. Janmey, P. A. (1994) *Annu. Rev. Physiol.* **56,** 169–191
33. Dos Remedios, C. G., Chhabra, D., Kekic, M., Dedova, I. V., Tsubakihara, M., Berry, D. A., and Nosworthy, N. J. (2003) *Physiol. Rev.* **83,** 433–473I. V.
34. Kwiatkowski, D. J. (1999) *Curr. Opin. Cell Biol.* **11,** 103–108
35. Azuma, T., Witke, W., Stossel, T. P., Hartwig, J. H., and Kwiatkowski, D. J. (1998) *EMBO J.* **17,** 1362–1370
36. Hartwig, J. H., Bokoch, G. M., Carpenter, C. L., Janmey, P. A., Taylor, L. A., Toker, A., and Stossel, T. P. (1995) *Cell* **82,** 643–653
37. Janmey, P. A., and Stossel, T. P. (1987) *Nature* **325,** 362–364
38. Kwiatkowski, D. J., Janmey, P. A., and Yin, H. L. (1989) *J. Cell Biol.* **108,** 1717–1726
39. Lueck, A., Brown, D., and Kwiatkowski, D. J. (1998) *J. Cell Sci.* **111,** 3633–3643
40. Cabello-Agueros, J. F., Hernandez-Gonzalez, E. O., and Mujica, A. (2003) *Cell Motil. Cytoskeleton* **56,** 94–108
41. Biswas, R. S., Baker, D. A., Hruska, K. A., and Chellaiah, M. A. (2004) *BMC Cell Biol.* http://www.biomedcentral.com/1471-2121/5/19
42. Breton, S., Nsumu, N. N., Galli, T., Sabolic, I., Smith, P. J., and Brown, D. (2000) *Am. J. Physiol.* **278,** F717–F725
43. Breton, S., Smith, P. J., Lui, B., and Brown, D. (1996) *Nat. Med.* **2,** 470–472
44. Brown, D., Lui, B., Gluck, S., and Sabolic, I. (1992) *Am. J. Physiol.* **263,** C913–C916
45. Brown, D., Hirsch, S., and Gluck, S. (1988) *J. Clin. Investig.* **82,** 2114–2126
46. Gluck, S. L., Lee, B. S., Wang, S. P., Underhill, D., Nemoto, J., and Holliday, L. S. (1998) *Acta Physiol. Scand. Suppl.* **643,** 203–212
47. Lee, B. S., Holliday, L. S., Ojikutu, B., Krits, I., and Gluck, S. L. (1996) *Am. J. Physiol.* **270,** C382–C388
48. Brown, D., and Breton, S. (2000) *J. Exp. Biol.* **203,** 137–145
49. Wagner, C. A., Finberg, K. E., Breton, S., Marshansky, V., Brown, D., and Geibel, J. P. (2004) *Physiol. Rev.* **84,** 1263–1314
50. Sun-Wada, G. H., Wada, Y., and Futai, M. (2004) *Biochim. Biophys. Acta* **1658,** 106–114
51. Brown, D., and Breton, S. (1996) *J. Exp. Biol.* **199,** 2345–2358
52. Toyomura, T., Oka, T., Yamaguchi, C., Wada, Y., and Futai, M. (2000) *J. Biol. Chem.* **275,** 8760–8765
53. Madsen, K. M., Verlander, J. W., Kim, J., and Tisher, C. C. (1991) *Kidney Int. Suppl.* **33,** S57–S63
54. Steinmetz, P. R. (1986) *Am. J. Physiol.* **251,** F173–F187
55. Lee, B. S., Gluck, S. L., and Holliday, L. S. (1999) *J. Biol. Chem.* **274,** 29164–29171
56. Chen, S. H., Bubb, M. R., Yarmola, E. G., Zuo, J., Jiang, J., Lee, B. S., Lu, M., Gluck, S. L., Hurst, I. R., and Holliday, L. S. (2004) *J. Biol. Chem.* **279,** 7988–7998
57. Vitavska, O., Wieczorek, H., and Merzendorfer, H. (2003) *J. Biol. Chem.* **278,** 18499–18505
58. Holliday, L. S., Lu, M., Lee, B. S., Nelson, R. D., Solivan, S., Zhang, L., and Gluck, S. L. (2000) *J. Biol. Chem.* **275,** 32331–32337
59. Breton, S., Wiederhold, T., Marshansky, V., Nsumu, N. N., Ramesh, V., and Brown, D. (2000) *J. Biol. Chem.* **275,** 18219–18224
60. Paunescu, T. G., Da Silva, N., Marshansky, V., McKee, M., Breton, S., and Brown, D. (2004) *Am. J. Physiol.* **287,** C149–C162
61. Weinman, E. J., Steplock, D., Tate, K., Hall, R. A., Spurney, R. F., and Shenolikar, S. (1998) *J. Clin. Investig.* **101,** 2199–2206
62. Shenolikar, S., and Weinman, E. J. (2001) *Am. J. Physiol.* **280,** F389–F395
63. Guilherme, A., Soriano, N. A., Bose, S., Holik, J., Bose, A., Pomerleau, D. P., Furcinitti, P., Leszyk, J., Corvera, S., and Czech, M. P. (2004) *J. Biol. Chem.* **279,** 10593–10605
64. Breton, S., Lisanti, M. P., Tyszkowski, R., McLaughlin, M., and Brown, D. (1998) *J. Histochem. Cytochem.* **46,** 205–214
65. Pastor-Soler, N., Beaulieu, V., Litvin, T. N., Da Silva, N., Chen, Y., Brown, D., Buck, J., Levin, L. R., and Breton, S. (2003) *J. Biol. Chem.* **278,** 49523–49529
66. Brown, D., Lydon, J., McLaughlin, M., Stuart-Tilley, A., Tyszkowski, R., and Alper, S. (1996) *Histochem. Cell Biol.* **105,** 261–267
67. Breton, S., Hammar, K., Smith, P. J. S., and Brown, D. (1998) *Am. J. Physiol.* **275,** C1134–C1142
68. Cunningham, C. C., Vegners, R., Bucki, R., Funaki, M., Korde, N., Hartwig, J. H., Stossel, T. P., and Janmey, P. A. (2001) *J. Biol. Chem.* **276,** 43390–43399
69. Stevens, A. L., Breton, S., Gustafson, C. E., Bouley, R., Nelson, R. D., Kohan, D. E., and Brown, D. (2000) *Am. J. Physiol.* **278,** C791–C802
70. Shurety, W., Stewart, N. L., and Stow, J. L. (1998) *Mol. Biol. Cell* **9,** 957–975
71. Kwiatkowski, D. J., Stossel, T. P., Orkin, S. H., Mole, J. E., Colten, H. R., and

Yin, H. L. (1986) *Nature* **323,** 455–458
72. Pastor-Soler, N., Isnard-Bagnis, C., Herak-Kramberger, C., Sabolic, I., Van Hoek, A., Brown, D., and Breton, S. (2002) *Biol. Reprod.* **66,** 1716–1722
73. Sun, H., Lin, K., and Yin, H. L. (1997) *J. Cell Biol.* **138,** 811–820
74. Banno, Y., Nakashima, T., Kumada, T., Ebisawa, K., Nonomura, Y., and Nozawa, Y. (1992) *J. Biol. Chem.* **267,** 6488–6494
75. Schwartz, J. H., Masino, S. A., Nichols, R. D., and Alexander, E. A. (1994) *Am. J. Physiol.* **266,** F94–F101
76. Cannon, C., van Adelsberg, J., Kelly, S., and Al-Awqati, Q. (1985) *Nature* **314,** 443–446
77. Litvin, T. N., Kamenetsky, M., Zarifyan, A., Buck, J., and Levin, L. R. (2003) *J. Biol. Chem.* **278,** 15922–15926
78. Lu, H., Sun, T. X., Bouley, R., Blackburn, K., McLaughlin, M., and Brown, D. (2004) *Am. J. Physiol.* **286,** F233–F243
79. Sun, T. X., Van Hoek, A., Huang, Y., Bouley, R., McLaughlin, M., and Brown, D. (2002) *Am. J. Physiol.* **282,** F998–F1011
80. Gundelfinger, E. D., Kessels, M. M., and Qualmann, B. (2003) *Nat. Rev. Mol. Cell Biol.* **4,** 127–139
81. Szaszi, K., Kurashima, K., Kaibuchi, K., Grinstein, S., and Orlowski, J. (2001) *J. Biol. Chem.* **276,** 40761–40768
82. Shapiro, M., Matthews, J., Hecht, G., Delp, C., and Madara, J. L. (1991) *J. Clin. Investig.* **87,** 1903–1909
83. Wu, M. S., Bens, M., Cluzeaud, F., and Vandewalle, A. (1994) *J. Membr. Biol.* **142,** 323–336
84. Reshkin, S. J., and Murer, H. (1992) *Am. J. Physiol.* **262,** F572–F577
85. Prat, A. G., Cunningham, C. C., Jackson, G. R., Jr., Borkan, S. C., Wang, Y., Ausiello, D. A., and Cantiello, H. F. (1999) *Am. J. Physiol.* **277,** C1160–C1169
86. Tamma, G., Klussmann, E., Procino, G., Svelto, M., Rosenthal, W., and Valenti, G. (2003) *J. Cell Sci.* **116,** 1519–1525
87. Lin, K. M., Wenegieme, E., Lu, P. J., Chen, C. S., and Yin, H. L. (1997) *J. Biol. Chem.* **272,** 20443–20450
88. Yin, H. L., and Stossel, T. P. (1979) *Nature* **281,** 583–586
89. Kumar, N., and Khurana, S. (2004) *J. Biol. Chem.* **279,** 24915–24918
90. Arpin, M., Pringault, E., Finidori, J., Garcia, A., Jeltsch, J. M., Vandekerckhove, J., and Louvard, D. (1988) *J. Cell Biol.* **107,** 1759–1766
91. Finidori, J., Friederich, E., Kwiatkowski, D. J., and Louvard, D. (1992) *J. Cell Biol.* **116,** 1145–1155
92. Lamb, J. A., Allen, P. G., Tuan, B. Y., and Janmey, P. A. (1993) *J. Biol. Chem.* **268,** 8999–9004